Supramolecular Chemistry
Publication details, including instructions for authors and subscription information:
http://www.informaworld.com/smpp/title~content=t713649759

Supramolecular assembly of lysine-b-glycine block copolypeptides at different solution conditions

Jeffery Gaspard[a]; James A. Silas[a]; Daniel F. Shantz[a]; Jeng-Shiung Jan[b]
[a] Artie McFerrin Department of Chemical Engineering, Texas A&M University, College Station, TX, USA [b] Department of Chemical Engineering, National Cheng Kung University, Tainan City, Taiwan, ROC

First published on: 20 August 2009

To cite this Article Gaspard, Jeffery , Silas, James A. , Shantz, Daniel F. and Jan, Jeng-Shiung(2010) 'Supramolecular assembly of lysine-b-glycine block copolypeptides at different solution conditions', Supramolecular Chemistry, 22: 3, 178 — 185, First published on: 20 August 2009 (iFirst)
To link to this Article: DOI: 10.1080/10610270903089746
URL: http://dx.doi.org/10.1080/10610270903089746

Supramolecular Chemistry
Vol. 22, No. 3, March 2010, 178–185

Taylor & Francis
Taylor & Francis Group

Supramolecular assembly of lysine-b-glycine block copolypeptides at different solution conditions

Jeffery Gaspard[a], James A. Silas[a], Daniel F. Shantz[a] and Jeng-Shiung Jan[b]*

[a]*Artie McFerrin Department of Chemical Engineering, Texas A&M University, Mail Stop 3122, College Station, TX 77843-3122, USA;* [b]*Department of Chemical Engineering, National Cheng Kung University, No. 1 University Road, Tainan City 701, Taiwan, ROC*

(*Received 4 March 2009; final version received 22 May 2009*)

Here we report the supramolecular assembly of poly(L-lysine)-*b*-polyglycine diblock copolypeptides at different solution conditions. Light scattering and confocal microscopy indicate that the supramolecular aggregates initially formed in solution are vesicles with a broad size distribution, depending strongly on the initial processing conditions. The vesicles formed after multiple pH cycles appear independent of the initial processing conditions and are related to the thermodynamic nature of the assembled supramolecular aggregates. Circular dichroism results verify that this change in size observed over pH cyclings tracks with the conformation changes of the lysine block confined in the vesicle membranes. This appears interesting for peptosome-based materials, implying a high level of fluidity in the membrane that allows the supramolecular aggregates formed in solution to respond to changes in pH. The results also show that the external stimulus, which is the change of pH in this study, provides an additional means to regulate polypeptide vesicle size and size distribution.

Keywords: polypeptides; vesicles; pH-responsive

Introduction

There have been significant advances in the last 10 years in the synthesis of 'hybrid' block copolymers wherein one block is a poly-α-amino acid and the other a 'conventional' polymer (e.g. polystyrene, polybutadiene, PEG) as well as block copolypeptides. The synthesis schemes of these block copolymers via *N*-carboxyanhydride (NCA) polymerisation were reviewed by Deming (*1*). These materials possess the structures and functions of proteins due to incorporation of amino acids, and have been shown to self-assemble into structures including vesicles (*2–13*), micelles (*6*, *13–18*) and hydrogels (*19–21*). Among these self-assembled structures, peptide-based vesicles are promising drug carriers and biomimetic encapsulants for trapping water-soluble drugs and solutes with capability to release them in response to external stimuli. Several studies have reported the pH-responsive properties of polypeptide-based vesicles (*2–7*, *12*, *13*) and demonstrated that the changes in chain conformation in the polypeptide domain can influence the vesicle formation and size.

The formation of vesicles can be prepared by those methods reported for liposome preparation and the decrease in the size distribution of vesicle dispersions can be achieved through several methods such as sonication, extrusion, vortexing and freeze–thaw cycles, or a combination of these methods (*22*). Vesicle extrusion is an effective means to allow fine adjustment of vesicle diameter to a desirable size for specific applications. Recently, this technique was used to prepare stable polypeptide vesicles with controllable diameter (*8*). However, it is worth to note that these polypeptide vesicles could be perturbed by the changes in solution conditions due to their stimuli-responsive properties as a result of the change in assembled structure and/or vesicle size.

In order to understand how external stimuli influence the assembled structure and/or size of polypeptide vesicles, we chose amphiphilic poly(L-lysine)-*b*-polyglycine diblock copolypeptides that form vesicles in aqueous solution for this study and the external stimulus is the change of pH in solution which can induce conformation changes in poly-L-lysine (i.e. coil–helix transitions). Polyglycine was chosen as the hydrophobic block in the current work in lieu of other hydrophobic amino acids for two reasons. First, in contrast to homopolypeptides of amino acids such as alanine, valine or leucine, glycine will not adopt a well-defined conformation. Second, polyglycine is less hydrophobic than most other hydrophobic amino acids which should allow vesicle membranes to be considerably more flexible and compliant. The second point is central to the work below, as it was desired to synthesise polymers capable of forming supramolecular aggregates wherein the hydrophobic block will enable the vesicle membranes to possess some level of fluidity.

*Corresponding author. Email: jsjan@mail.ncku.edu.tw

ISSN 1061-0278 print/ISSN 1029-0478 online

DOI: 10.1080/10610270903089746
http://www.informaworld.com

Four different preparation methods were used for the preparation of vesicles formed by poly(L-lysine)-*b*-polyglycine diblock copolypeptides in solution with different diameters ranging from sub- to several micrometres. After processing by multiple pH cycles, these assembled vesicles are very similar in size despite a variety of initial preparation approaches. The vesicles formed after multiple pH cycles are related to the thermodynamic nature of the assembled supramolecular aggregates. The vesicular assemblies show dynamic properties indicating that the membrane bilayer possesses a high level of fluidity. The results also show that the changes of pH in this study provide an additional means to regulate vesicle size and size distribution.

Experimental

Block copolypeptide synthesis

N_ε-Z-L-lysine (Z-Lys, ~99%, Z: carboxybenzyl; Fluka, Milwaukee, WI, USA) and glycine (Gly, 99%; Aldrich, St Louis, MO, USA) were used as received. THF (ACS Reagent, Aldrich) and diethyl ether (anhydrous; ACS Reagent, VWR, West Chester, PA, USA) were dried using Na metal. Hexane (ACS Reagent, EM Science, Gibbstown, NJ, USA) was dried using calcium hydride. Triphosgene (98%; Aldrich) was used as received, as was 2,2′-bipyridyl (99 + %; Aldrich) and bis(1,5-cyclooctadiene) nickel (0) (98 + %; Strem, Newburyport, MA, USA). A solution of 1.0 M HCl in diethyl ether and 33 wt% HBr in acetic acid were used as received from Aldrich. The monomer synthesis and polypeptide synthesis were performed on a Schlenk line using standard procedures. The nickel initiator 2,2′-bipyridyl-Ni(1,5-cyclooctadiene) (BpyNiCOD) was prepared in a glove box by ligand exchange of the Ni-bis(COD) complex in the presence of 2,2′-bipyridyl in ether using the procedure described by Binger and coworkers (*23*). The Z-Lys and Gly NCAs were synthesised in dry THF using triphosgene as described by Daly and Poché (*24*).

Diblock and triblock copolypeptides were synthesised using N_ε-Z-protected L-lysine and glycine NCAs using the procedure developed by Deming (*25–27*). The polypeptides were then dialysed and lyophilised. ^{1}H NMR of the protected copolypeptide in *d*-TFA was used to verify the composition of the copolypeptide, and gel permeation chromatography was used to determine the molecular weight and polydispersity (Styragel HR4 column, effluent: 10 mM LiBr in DMF, Standard: PEO). The notation used throughout for the block copolypeptides is Lys_n-*b*-Gly_m, where *m* and *n* are the number of amino acids in the respective blocks. Below, a detailed description of the synthesis procedures is given for a specific diblock copolypeptide, Lys_{110}-*b*-Gly_{55}.

Poly(Z-Lys)$_{110}$-b-poly(glycine)$_{55}$

In the glove box, Z-Lys NCA (1.53 g, 5 mmol) and BpyNiCOD (81 mg, 0.025 mmol) were weighed out, placed in 100 ml flasks and removed from the glove box. Dry THF (~25 ml for Z-Lys NCA and ~8 ml for BpyNiCOD) was transferred to the two flasks using a Schlenk line. The BpyNiCOD solution was then transferred to the Z-Lys NCA solution through a cannula under argon atmosphere. Immediately after addition of the BpyNiCOD solution, the flask was stirred for 16 h. Gly NCA (0.25 g, 2.5 mmol) was weighed out, dissolved in THF (~15 ml) and added to the reaction mixture. After stirring for an additional 16 h, the polypeptide was isolated by adding diethyl ether containing 1 mM HCl to the reaction mixture, causing precipitation of the polypeptide. The polypeptide was dried in vacuum to give a white solid.

Poly(L-lysine)$_{110}$-b-poly(glycine)$_{55}$

Poly(Z-Lys)$_{110}$-*b*-poly(glycine)$_{55}$ (0.3 g) was dissolved in trifluoroacetic acid (15 ml) in a 100 ml flask. Once all polypeptides were in solution, excess 33 wt% HBr in acetic acid was added via syringe (~0.9 ml). The solution was left to stir for 20 min and then diethyl ether (80 ml) was added to precipitate the polypeptide. The polypeptide was collected via centrifugation, dried in vacuum and dissolved in deionised (DI) water (40 ml). Once the polypeptide was in solution, the solution was transferred to a dialysis tubing cellulose membrane (MWCO 12,400; Sigma, St Louis, MO, USA) and the membrane was placed in a 10 L container of DI water. The water was exchanged two to three times per day over the next 3 days. The solution was then placed on a freeze dryer to yield the product as a white spongy material. Typical polypeptide yields were between 75 and 85% based on the NCA.

Preparation of vesicles

For the samples shown in Figure 2, the block copolypeptide was dissolved in DI water at a concentration of 1 mg/ml and then the solution was sonicated (power: 80 W) for 10 min. The solution pH was adjusted using 1 M NaOH solution and 1 M HCl solution. For the samples at pH 7 shown in Figure 3, the block copolypeptide was dissolved in methanol at a concentration of 5 mg/ml and then 250 μg of this solution was placed in a glass vial and the methanol was allowed to evaporate. This dry film was then exposed to 2 ml of a neutral aqueous solution (pH 7), resulting in vesicles forming off the surface. For the samples at pH 11 shown in Figure 3, the same vesicle solution was prepared in the same manner and followed by adjusting the pH to 11 using concentrated NaOH solution. A small amount of Nile Red, dissolved in methanol at a concentration of 0.1 mg/ml, was added for visualisation purposes. Nile Red was added, in a 1:5 molar ratio, in the

block copolypeptide dissolved in methanol and then allowed to evaporate. In Figure 4, the vesicles were prepared by exposing the dry film to 2 ml of a 300 mM NaCl solution. The pH of the solution was adjusted using 1 M NaOH in 300 mM NaCl solution and 1 M HCl in 300 mM NaCl solution. In Figure 5, the vesicles were prepared by rehydrating the dry film with a 100 mM sucrose solution and the mixtures were then extruded through a 80 nm filter (Whatman polycarbonate) nine times before analysis. For the samples shown in Figure 6, 50 μl of methanol solution (5 mg polypeptide/ml) was added to 2 ml of a 100 mM sucrose solution and then vortexed for 5 min. For the samples shown in Figures 5 and 6, the solution pH was adjusted using 1 M NaOH in 100 mM sucrose solution and 1 M HCl in 100 mM sucrose solution.

Characterisation

Gel permeation chromatography measurements were performed before deprotection of the polypeptides using a Shimadzu system consisting of one Styragel HR4 (Waters, Milford, MA, USA) column, eluted with 10 mM LiBr in DMF at 25°C. The eluent flow rate was 1 ml/min. Calibration was performed using poly(ethylene oxide) standards. ^{1}H NMR spectra were recorded at 300 MHz on a Mercury 300 Varian spectrometer using *d*-TFA as the solvent. Critical aggregation concentrations (cac) were determined by measuring the conductivity of block copolypeptide solutions as a function of polypeptide concentration (0.001 – 1 mg/ml). The conductivity measurements were performed with an Accumet AB30 conductivity meter with a conductivity cell (0.1 cm^{-1} cell constant). Dynamic light scattering (DLS) measurements were carried out using a Brookhaven ZetaPALS instrument. Vertically polarised light with a wavelength of 658 nm was used as the incident beam. The intensity of the scattered light was measured at a 90° scattering angle and the temperature was controlled at 25°C. Time-averaged particle size distributions were collected over an analysis time of at least 10 min. The hydrodynamic radius (R_h) and polydispersity of the polypeptide supramolecular structures were determined from LS experiments using Brookhaven Instruments Dynamic LS software (CONTIN analysis). LS measurements at different angles were performed with a Brookhaven Instruments BI-200SM goniometer using a Melles Griot HeNe laser with a wavelength of 632.8 nm. The scattered intensity was measured at several angles between 30° and 130°. Circular dichroism (CD) measurements were performed with a AVIV stopped flow circular dichroism spectrometer model 202SF. CD measurements were performed on block copolypeptide solutions above and below the cac, using 0.01 – 0.5 N NaOH and HCl solutions to adjust the pH to keep the block copolypeptide concentrations within the desired range. Confocal images were obtained with a Leica TCS SP5 broad band confocal microscope (Bannockburn, IL, USA) and analysed with ImageJ (National Institute of Health, Bethesda, MD, USA). A 3/16th inch thick square rubber gasket is placed on top of a 22 × 50 mm glass cover slip as a sample holder. The preparation of those vesicle solutions was described in Section 'Poly(Z-Lys)$_{110}$-*b*-poly(glycine)$_{55}$' and then a threefold of slightly higher osmotic solution of phosphate buffer solution (300 – 310 mOsm/kg) was added to the vesicle solution for analysis using the 63× oil objective lens (NA = 1.25). The pictures were taken at a resolution of either 512 × 512 or 1024 × 1024, a refresh rate of 400 Hz, a pinhole size of 100 μm and a voltage of 700 V for the photomultiplier tube. The laser excitation/emission wavelength for Nile Red was 543/600 – 700 nm.

Results and discussion

Table 1 summarises the block copolypeptide molecular weights and composition as determined by GPC and ^{1}H NMR. As shown in previous work (*25*, *27*), the current synthesis methodology leads to polypeptides possessing a reasonably narrow molecular weight distribution. A representative GPC chromatogram and ^{1}H NMR spectrum of the Z-Lys$_{120}$-*b*-Gly$_{30}$ diblock copolypeptide are included in the Supporting Information as are the cac values. ^{1}H NMR of the polypeptide in *d*-TFA was performed to determine the compositions of the block copolypeptides, which were found to be within 5% of the predicted values based on the ratio of NCAs. The block ratio of Z-L-lysine: Gly was determined from the ratio of the peak intensity of α-hydrogen protons of Gly (CH_2: $\delta = 4.2$ ppm) and benzyl protons of Z-L-lysine ($COOCH_2$-C_6H_5: $\delta = 7.2$ ppm). After deprotection, the remaining Z groups in the block copolypeptides are well below 3% as determined by ^{1}H NMR. In the interest of space, what follows will focus on two block copolypeptides, Lys$_{200}$-*b*-Gly$_{50}$ and Lys$_{110}$-*b*-Gly$_{55}$.

It is well known that the coil – helix transition of poly-L-lysine occurs between pH 9 and 10 (*28*, *29*). Figure 1 shows the CD behaviour of the Lys$_{110}$-*b*-Gly$_{55}$ as a function of pH both above and below the cac. Below the cac, a clear random coil → α-helix transition is observed at pH 9.5.

Table 1. Composition, molecular weight and polydispersity of the block copolypeptides investigated.

Copolypeptide	M_n	M_W/M_n
Z-Lys$_{120}$-*b*-Gly$_{30}$	35,600	1.21
Z-Lys$_{200}$-*b*-Gly$_{50}$	53,500	1.17
Z-Lys$_{340}$-*b*-Gly$_{85}$	95,300	1.24
Z-Lys$_{110}$-*b*-Gly$_{55}$	31,800	1.20
Z-Lys$_{320}$-*b*-Gly$_{160}$	93,800	1.30
Z-Lys$_{400}$-*b*-Gly$_{200}$	118,200	1.09

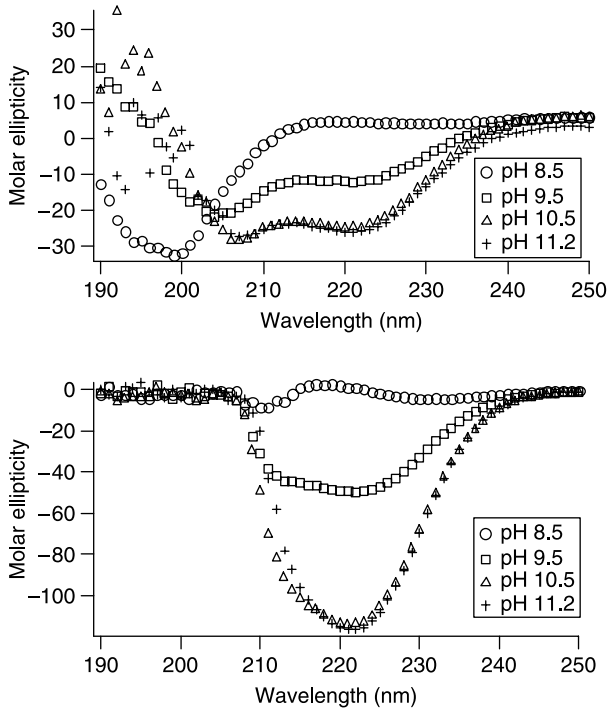

Figure 1. CD spectra of Lys_{110}-*b*-Gly_{55} from pH 8.5 to pH 11.2 at concentrations below (top, 1.16 μM) and above (bottom, 4.05 μM) the cac value.

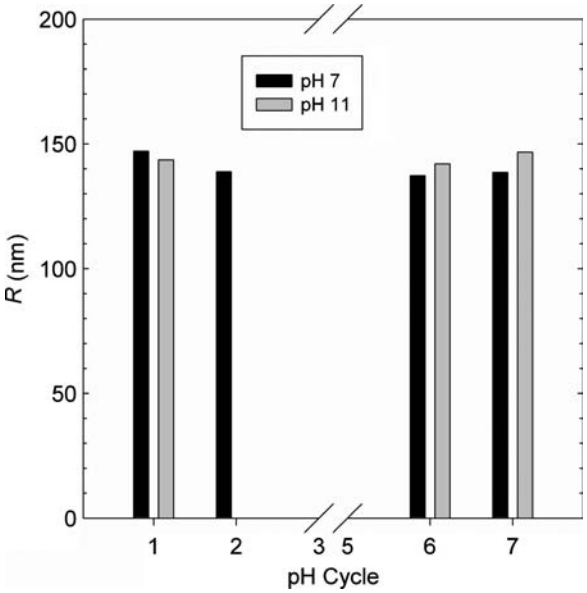

Figure 2. Plot of the radius of gyration (*R*) versus pH cycle for a solution containing Lys_{200}-*b*-Gly_{50}. This copolypeptide was first dissolved in DI water at neutral pH and followed by 10 min sonication.

By contrast, CD measurements above the cac values show that, at higher pH, the poly-L-lysine segments adopt a mixture of α-helix and β-sheet conformations. For other block copolypeptides, the lysine block also exhibits similar behaviour (not shown). It indicates that the self-assembly of block copolypeptides results in the confinement of poly-L-lysine segments and the confined poly-L-lysine segments exhibit different folding behaviours from free chains. According to our study, R_h is close to the radius of gyration (R_g) at high salt concentration as shown in the Supporting Information (Figure 2S). For 300 mM NaCl and 100 mM sucrose solutions, for which the osmotic pressure is about 300 mOsm/kg, we found R_h from DLS is very close to R_g from static light scattering (SLS) as well.

In order to investigate how the external stimuli, pH cycles and different preparation methods influence the assembled structure and/or size of polypeptide vesicles, the first method is to prepare the vesicles by directly dissolving block copolypeptides in DI water, followed by 10 min sonication. Figure 2 shows a plot of the radius of gyration versus 7 pH cycles between 7 and 11 for Lys_{200}-*b*-Gly_{50}. This block copolypeptide was first dissolved in DI water at neutral pH and the radius of gyration is 147 nm. From Figure 2, the result shows that the vesicle size did not change much upon pH changes. It indicates that the perturbation, folding/unfolding transition of the lysine block, has little influence on the vesicle size as well as on the number of aggregated Lys_{200}-*b*-Gly_{50} chains in a vesicle, and the vesicles are in equilibrium. Block copolypeptide solutions stored over 3 weeks were remeasured and the results are identical to that of freshly prepared solutions, indicating that the vesicles are stable in solution at neutral pH.

It is worth noting that at pH 11, the vesicles are initially well dispersed; over the time frame of hours, the vesicles aggregate and eventually precipitate from solution, and the rate of this increases with increasing molecular weight of the block copolypeptide. This can be understood as poly-L-lysine adopting an α-helix or a β-sheet conformation at pH 11 is less soluble than that adopting a coil conformation. Also, the solubility of helical or sheet-like lysine chains in aqueous solution decreases as the molecular weight of poly-L-lysine increases. This result, in a sense, is quite interesting, suggesting that the lysine block conformation can be used to reversibly change from highly aggregated/precipitated copolypeptides to well-defined vesicles (*vide infra*).

The second preparation method is thin film rehydration (*22*). The block copolypeptide was dissolved in methanol, deposited as a film onto a glass substrate and then rehydrated with an aqueous solution (pH 7) to result in vesicle formation. The initial assembled supramolecular aggregates formed are polydisperse and the size range of these supramolecular aggregates is from a few hundred nanometres to 10 μm (Figure 3S, Supporting Information), thus facilitating imaging using laser scanning confocal microscopy. From this method, there is no control on the curvature of bilayers formed by these amphiphilic block copolypeptides, which results in the broad size range

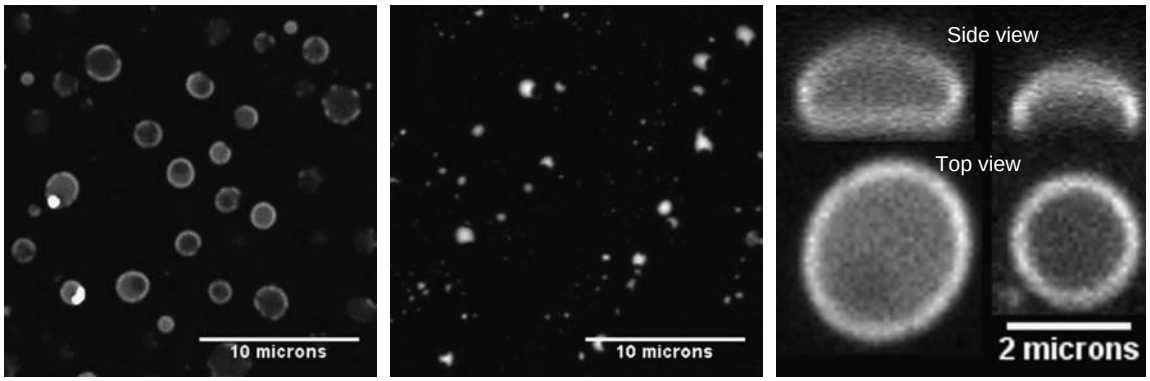

Figure 3. Confocal images of Lys_{200}-*b*-Gly_{50} vesicles formed (before pH cycling) by thin film rehydration at pH 7 (left and right) and pH 11 (middle) in the presence of Nile Red fluorescence.

of vesicles. Figure 3 shows confocal images of the assembled Lys_{200}-*b*-Gly_{50} supramolecular aggregates using the thin film rehydrate technique in the presence of Nile Red fluorescence at pH 7 and 11. From the left confocal image, the bright rings indicate the formation of micrometre-sized vesicles at pH 7. The right confocal image shows the side and top view of vesicles sitting on a glass substrate and indicates that they are unilamellar with no fluorescence intensity within the centres of the vesicles. Though it is not the most accurate method of detecting multiple membranes, the formation of unilamellar vesicles is very likely due to the highly charged nature of the membranes favouring intermembrane repulsion. For the supramolecular objects formed at pH 11, it is hard to determine whether they are vesicles or not probably due to the compaction of polypeptide chains in the supramolecular aggregates (the middle confocal image).

Then, the assembled vesicles formed in solution over numerous pH cycles were investigated. The Lys_{200}-*b*-Gly_{50} block copolypeptide was dissolved in methanol, deposited as a film onto a glass substrate and then rehydrated with a 300 mM NaCl solution to result in vesicle formation. The initial assembled supramolecular aggregates formed are polydisperse (polydispersity $\sim$ 1) and the size range of these supramolecular aggregates is from a few hundred nanometres to 10 μm (Figure 3S, Supporting Information). Figure 4 shows the radius of gyration of Lys_{200}-*b*-Gly_{50} vesicles formed as a function of the number of pH cycles. Previous studies showed that short lysine-b-leucine polypeptide vesicles disrupt after adding NaCl salt concentration greater than 500 mM due to the screening of intrachain and interchain electrostatic repulsions of the poly-L-lysine block (*8*). The preparation of vesicles using this method in this study ensures no osmotic stress between the inside and outside of the vesicles because there is no difference in NaCl concentration on both sides of vesicle membranes. From Figure 4, the vesicle size decreases dramatically to about 190 nm and, from confocal microscopy, the range of vesicle size is mostly between 100 and 600 nm after one cycle. Also, the polydispersity of these vesicles decreases after one cycle. It indicates that the perturbation, the folding/unfolding of the lysine block as well as the solubility change of the lysine block, decreases the number of aggregated Lys_{200}-*b*-Gly_{50} chains in one vesicle after the cycle and provides an alternative means to regulate vesicle size and size distribution other than sonication, extrusion, vortexing and freeze–thaw cycles. This relatively small energetic change, folding/unfolding (as well as the change of solubility) of the lysine block, provides a pathway for the relatively large changes in vesicle size and size distributions. It is also noteworthy that the conformation change of the lysine block results in the change

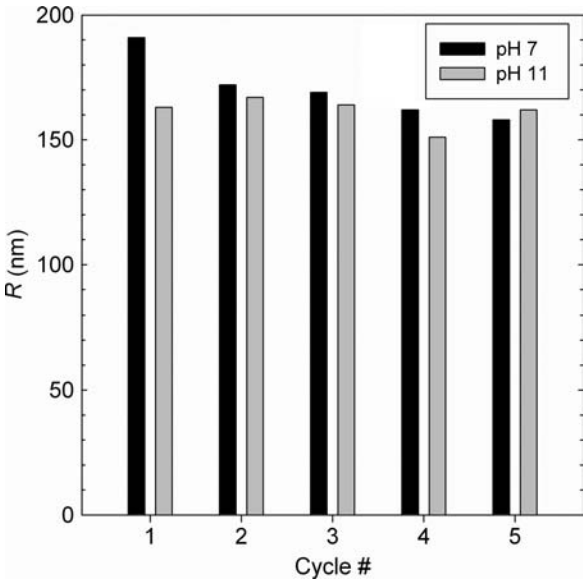

Figure 4. Plot of the radius of gyration (*R*) versus pH cycle for a solution containing Lys_{200}-*b*-Gly_{50} formed by budding vesicles of a surface by rehydrating the dry film of polypeptide with a 300 mM NaCl solution.

of solubility of the lysine block which, in turn, influences the self-assembly behaviour of these block copolypeptides. The aggregates at pH 11 are generally smaller than the aggregates formed at pH 7, probably due to a compaction of the lysine block as it goes through the folding/unfolding transition. Also, the values of the radius of gyration at pH 7 are slightly higher in cycles 1 and 2 and trend to approximately 155 ± 6 nm with low polydispersity (0.12 ± 0.02) after four cycles, very close to the values shown in Figure 2. Also, from confocal microscopy, the vesicle size is well below 400 nm and the relatively large vesicles (>500 nm) were not observed in solution.

To study this more closely, this same solution (i.e. the sample shown in Figure 4) was extruded through an 80 nm filter repeatedly (nine times) before pH cycling/SLS analysis, which is the third method. Liposome-based extrusion technique is an effective means to allow fine adjustment of vesicle diameter to a desirable size. We observed that aqueous suspension of Lys_{200}-*b*-Gly_{50} vesicles could easily be extruded through polycarbonate membranes. Deming and co-workers found that polypeptide vesicles, which are composed of the flexible hydrophilic block (e.g. poly-L-lysine or poly-L-glutamic acid) and poly-L-leucine, can be extruded without difficulty as well (*8*, *9*). It shows that the membranes of these vesicles are considerably flexible and compliant. For comparison, they found that the as-formed micrometre-sized vesicles of rod–rod block copolypeptides could not be reduced in size by extrusion probably due to the rigidity of the membrane (*7*).

Figure 5 shows the size variation of Lys_{200}-*b*-Gly_{50} vesicles over several pH cycles. Instead, here the initial aggregates are markedly smaller ($R = 45$ nm at pH 7), but again trend to similar values (143 ± 8 nm) as the samples shown in Figure 2 after five pH cycles. It shows that the size of these extruded polypeptide vesicles increases due to the folding/unfolding of the lysine block as well as the solubility change of the lysine block. The conformation and solubility change of the lysine block regulates the number of aggregated polypeptide chains in a vesicle and results in increasing of the vesicle size, which is the increase in the number of aggregated polypeptide chains. Again, the conformation change of the lysine block results in the change of solubility of the lysine block which, in turn, influences the self-assembly behaviour of these block copolypeptides. The aggregates at pH 11 are generally larger than the aggregates formed at pH 7, probably due to the aggregation of the vesicles or the increase in the number of aggregated polypeptide chains in a vesicle. From confocal microscopy, the vesicle size is well below 400 nm and no large vesicles (>500 nm) were observed in solution at each cycle. From DLS measurements, polydispersity of these vesicles at pH 7 was low (0.13 ± 0.03) and did not change much after four cycles.

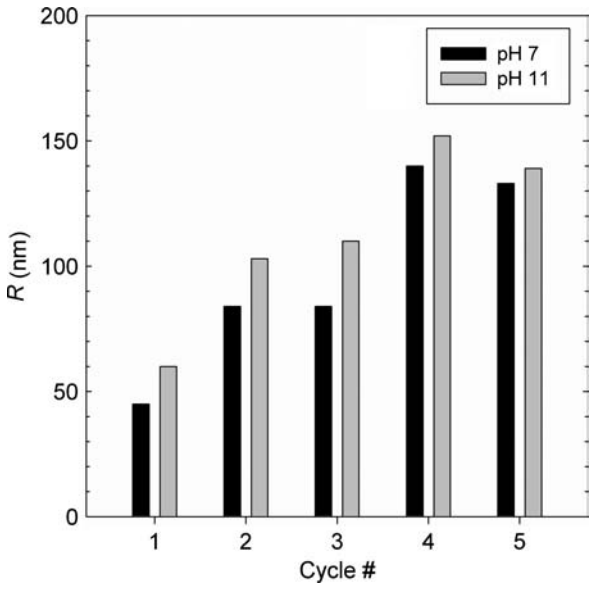

Figure 5. Plot of the radius of gyration (R) versus pH cycle for a solution containing Lys_{200}-*b*-Gly_{50} formed by budding vesicles of a surface followed by multiple extrusions through a 80 nm filter.

These results are consistent with the idea that multiple pH cycles result in vesicles that have comparable size distributions to those shown in Figure 2.

Finally, the fourth method is solvent displacement (*22*). Vesicles were prepared wherein the polypeptides were dissolved in methanol, and then this solution was added to a 100 mM sucrose solution and then vortexed for 5 min. The resulting solution contained 2.5 v/v% of methanol. The preparation of vesicles using the fourth method ensures no osmotic stress between the inside and outside of the vesicles because there is no difference in sucrose concentration on both sides of the vesicle membrane. Confocal microscopy confirmed that Lys_{200}-*b*-Gly_{50} vesicles retain their spherical shape in the presence of 100 mM sucrose concentration (not shown). Previous studies showed that short lysine-b-leucine vesicles were found to flatten and wrinkle after adding saturated sucrose solution (250 mM) due to the loss of water from the vesicle interiors in response to the osmotic pressure (*8*).

Figure 6 shows the radius of gyration of Lys_{200}-*b*-Gly_{50} vesicles prepared by the fourth method as a function of the pH cycle. It is observed that, similar to the results for the initially extruded vesicles (the third method), the initial vesicles are small (~110 nm at pH 7) but over four pH cycles trend to a radius of gyration of approximately 147 ± 4 nm. From DLS measurements, polydispersity of these vesicles at pH 7 in this case gradually decreases after each cycle and the polydispersity is 0.12 ± 0.03 after four cycles. Again, from confocal microscopy, the vesicle size is well below 400 nm and no large vesicles (>500 nm)

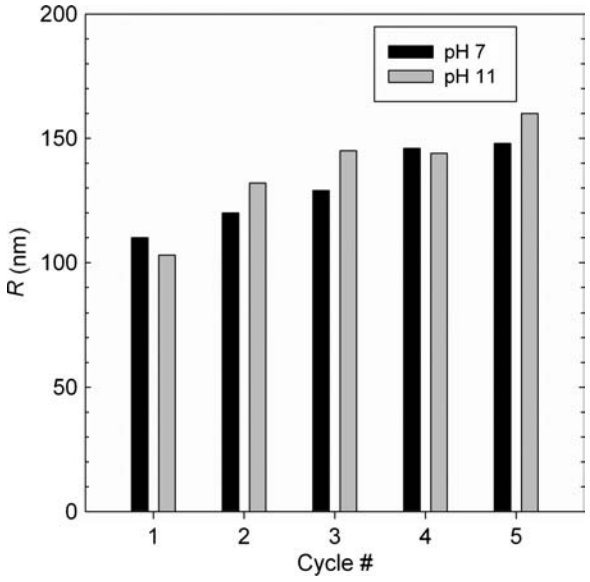

Figure 6. Plot of the radius of gyration (R) versus pH cycle for a solution containing Lys_{200}-*b*-Gly_{50} vesicles formed by dissolving polypeptide in methanol followed by addition to a 100 mM sucrose solution and vortexing.

were observed in solution at each cycle. Again, these results are consistent with the idea that multiple pH cycles result in vesicles that have comparable size distributions to those shown in Figure 2. What appears to cause this behaviour is the change in conformation and solubility of the lysine block, and that this relatively small energetic change can regulate vesicle size. The state of the vesicles reaches equilibrium after multiple pH cycles and is ultimately independent of their preparation method.

Reinecke and Doebereiner reported the morphology of block copolymer vesicles which is determined by the bending elastic energy of their bilayer membrane. Forces acting on the membrane establish a local mechanical equilibrium, though the individual polymer vesicles are not in equilibrium with the bulk (*30*). This explains that the vesicles initially formed in solution using different preparation methods result in vesicles with different sizes and size distributions. Also, Eisenberg group demonstrated that the thermodynamic stabilisation of block copolymer vesicles is based on the segregation of the hydrophilic chains by the block length between the inside and outside of the vesicles. If the vesicles are to be thermodynamically stable, the curvature of the vesicles needs to be stabilised by having the long hydrophilic chains segregate to the outside of the vesicle, while the short hydrophilic chains segregate to the inside. Thus, the repulsion among corona chains outside is stronger than that inside the vesicles, and the curvature is maintained in a thermodynamically stable manner (*31*, *32*). In this study, the vesicles formed after multiple pH cycles appear independent of the initial processing conditions and are related to the thermodynamic nature of the assembled supramolecular aggregates. This indicates that the preferential segregation of the hydrophilic chains by the block length between the inside and outside of the vesicles reaches an equilibrium-like state, which results in the curvature stabilisation of the membrane bilayer, and thus sustains the thermodynamically stable polypeptide vesicles. These block copolypeptides with a polydispersity index between 1.1 and 1.3 are not monodispersed, which suggests the occurrence of the preferential segregation of the hydrophilic chains by the block length between the inside and outside of the vesicles.

This work illustrates that after multiple pH cycles, these vesicles prepared by using four different methods all approach very similar sizes/structures. The results show that these block copolypeptides form supramolecular aggregates in solution that are non-glassy and solution-responsive, and ultimately reaches equilibrium after multiple pH cycles. Moreover, the driving force for this appears to be the change in conformation (i.e. folding/unfolding) and solubility of the lysine block, as the change in vesicle size and size distribution occurs over pH cycles.

Conclusions

Here, the self-organisation of poly(L-lysine)-*b*-polyglycine diblock copolypeptides at different processing and solution conditions is reported. Four different preparation methods were employed to afford the self-assembly of block copolypeptides in solution. The supramolecular aggregates initially formed in solution are vesicles whose size, ranging from 50 nm to several micrometres, depends strongly on the initial preparation methods. The vesicles formed after multiple pH cycles appear essentially independent of the initial processing conditions. This change in size observed over pH cyclings tracks with the reversible folding/unfolding of the lysine block confined in the vesicle membranes. The conformation change of the lysine block results in the solubility change of the lysine block which, in turn, influences the self-assembly behaviour of these block copolypeptides as well. Thus, it indicates that a very small change in free energy leads to dramatically large changes in vesicle size and size distribution. It is also worth to note that the confined poly-L-lysine segments exhibit different folding behaviours from free chains. The non-glassy nature of the vesicles is evidenced by observing their behaviour in solution over numerous pH cycles. The result implies that the membrane bilayer possesses a high level of fluidity that allows the aggregates formed in solution to respond to changes in pH. The results also show that the changes of pH in this study provide an alternative means to regulate polypeptide vesicle size and size distribution other than sonication, extrusion, vortexing and freeze–thaw cycles.

Acknowledgements

J.-S. Jan acknowledges start-up support from the National Cheng Kung University. J.-S. Jan and D.F. Shantz also acknowledge financial support from the Texas A&M University Life Science Task Force and Robert A. Welch Foundation (A-1638), J.M. Scholtz for access to the CD instrument, and the Chemistry Department at Texas A&M for access to the NMR facilities.

Supporting information available

Table listing the polypeptide molecular weights determined by GPC, cac of the polypeptides, GPC chromatogram and ^{1}H NMR spectrum of representative polypeptide sample.

References

(1) Deming, T.J. *Adv. Polym. Sci.* **1997**, *390*, 386–389.
(2) Checot, F.; Lecommandoux, S.; Gnanou, Y.; Klok, H.A. *Angew. Chem. Int. Ed.* **2002**, *41*, 1339–1343.
(3) Checot, F.; Lecommandoux, S.; Klok, H.A.; Gnanou, Y. *Eur. Phys. J. E* **2003**, *10*, 25–35.
(4) Kukula, H.; Schlaad, H.; Antonietti, M.; Foerster, S. *J. Am. Chem. Soc.* **2002**, *124*, 1658–1663.
(5) Rodriguez-Hernandez, J.; Lecommandoux, S. *J. Am. Chem. Soc.* **2005**, *127*, 2026–2027.
(6) Checot, F.; Brulet, A.; Oberdisse, J.; Gnanou, Y.; Mondain-Monoval, O.; Lecommandoux, S. *Langmuir* **2005**, *21*, 4308–4315.
(7) Bellomo, E.G.; Wyrsta, M.D.; Pakstis, L.; Pochan, D.L.; Deming, T.J. *Nat. Mater.* **2004**, *3*, 244–248.
(8) Holowka, E.P.; Pochan, D.J.; Deming, T.J. *J. Am. Chem. Soc.* **2005**, *127*, 12423–12428.
(9) Holowka, E.P.; Sun, V.Z.; Kamei, D.T.; Deming, T.J. *Nat. Mater.* **2007**, *6*, 52–57.
(10) Checot, F.; Rodriguez-Hernandez, J.; Gnanou, Y.; Lecommandoux, S. *Biomol. Eng.* **2007**, *24*, 81–85.
(11) Sun, J.; Chen, X.S.; Deng, C.; Yu, H.J.; Xie, Z.G.; Jing, X.B. *Langmuir* **2007**, *23*, 8308–8315.
(12) Tian, Z.; Wang, M.; Zhang, A.Y.; Feng, Z.G. *Polymer* **2008**, *49*, 446–454.
(13) Huang, C.J.; Chan, F.C. *Macromolecules* **2008**, *41*, 7041–7052.
(14) Harada, A.; Cammas, S.; Kataoka, K. *Macromolecules* **1996**, *29*, 6183–6188.
(15) Cho, C.S.; Nah, J.W.; Jeong, Y.I.; Cheon, J.B.; Asayama, S.; Ise, H.; Akaike, T. *Polymer* **1999**, *40*, 6769–6775.
(16) Babin, J.; Rodriguez-Hernandez, J.; Lecommandoux, S.; Klok, H.A.; Achard, M.-F. *Faraday Discuss.* **2005**, *128*, 179–192.
(17) Agut, W.; Brulet, A.; Taton, D.; Lecommandoux, S. *Langmuir* **2007**, *23*, 11526–11533.
(18) Zhao, C.W.; Zhuang, X.L.; He, C.L.; Chen, X.S.; Jing, X.B. *Macromol. Rapid Commun.* **2008**, *29*, 1810–1816.
(19) Nowak, A.P.; Sato, J.; Breedveld, V.; Deming, T.J. *Supramol. Chem.* **2006**, *18*, 423–427.
(20) Breedveld, V.; Nowak, A.P.; Sato, J.; Deming, T.J.; Pine, D.J. *Macromolecules* **2004**, *37*, 3943–3953.
(21) Nowak, A.P.; Breedveld, V.; Pakstis, L.; Ozbas, B.; Pine, D.J.; Pochan, D.J.; Deming, T.J. *Nature* **2002**, *417*, 424–428.
(22) Kita-Tokarczyk, K.; Grumelard, J.; Haefele, T.; Meier, W. *Polymer* **2005**, *46*, 3540–3563.
(23) Binger, P.; Doyle, M.J.; McMeeking, J.; Krueger, C.; Tsay, Y.-H. *J. Organometal. Chem.* **1977**, *135*, 405–414.
(24) Daly, W.H.; Poché, D. *Tetrahedron Lett.* **1988**, *29*, 5859–5862.
(25) Deming, T.J. *Nature* **1997**, *390*, 386–389.
(26) Deming, T.J. *J. Am. Chem. Soc.* **1998**, *120*, 4240–4241.
(27) Deming, T.J.; Curtin, S.A. *J. Am. Chem. Soc.* **2000**, *122*, 5710–5717.
(28) Davidson, B.; Fasman, G.D. *Biochemistry* **1967**, *6*, 1616–1629.
(29) Greenfield, N.; Fasman, G.D. *Biochemistry* **1969**, *8*, 4108–4116.
(30) Reinecke, A.A.; Doebereiner, H.-G. *Langmuir* **2003**, *19*, 605–608.
(31) Luo, L.; Eisenberg, A. *J. Am. Chem. Soc.* **2001**, *123*, 1012–1013.
(32) Luo, L.; Eisenberg, A. *Langmuir* **2001**, *17*, 6804–6811.